Talanta 84 (2011) 881–886

Contents lists available at ScienceDirect

Talanta

journal homepage: www.elsevier.com/locate/talanta

Site-selective probe for investigating the asynchronous unfolding of domains in bovine serum albumin

Hai Wu, Po Wang, Xiao Hu, Zong Dai*, Xiaoyong Zou*

School of Chemistry and Chemical Engineering, Sun Yat-Sen University, Guangzhou 510275, PR China

ARTICLE INFO

Article history:
Received 10 December 2010
Received in revised form 9 February 2011
Accepted 16 February 2011
Available online 23 February 2011

Keywords:
Bovine serum albumin
Alizarin red S
Asynchronous unfolding
Visualization
Electrochemistry

ABSTRACT

A convenient method is proposed for precise investigation of the asynchronous structural transition of the domains in bovine serum albumin (BSA) during unfolding process. The method is based on a site-selective probe, alizarin red S (ARS), which has a high affinity to the subdomain IIA of BSA. BSA–ARS complex was formed and gradually unfolded by urea from 0 to 8.0 M. The unfolding occurred in different domains of BSA resulted in distinct alterations of the microenvironment of the bound ARS. The spectral response of BSA–ARS complex, including the color, the UV absorption at 530 and 432 nm, and the intrinsic fluorescence at 342 and 310 nm with the excitation wavelength of 280 nm, showed slight changes in the urea concentration from 0 to 4.5 M, drastic changes from 4.5 to 6.0 M, and almost no changes from 6.0 to 8.0 M. The redox behavior of bound ARS between 0.3 and 0.8 V also showed the same trend. Consequently, a two-step, three-state transition process was monitored by naked eyes, UV–vis spectroscopy and electrochemistry. It is the first report to realize the indicator of the intermediate state during the unfolding process of BSA through convenient methods instead of expensive approaches. The work provides a facile method for the investigation of the unfolding process of multidomain proteins.

1. Introduction

The three-dimensional structure of a protein is responsible for its biological activity. Structural alterations, namely the unfolding or denaturation of proteins, frequently result in the loss of activity and a wide range of diseases [1,2]. Therefore, the precise and convenient elucidation of the folding/unfolding of a protein, especially the complex protein contains multidomain structures in which each domain can unfold dependently or independently, is of great biological importance and one of the principal challenges for modern biophysics [3,4].

Bovine serum albumin (BSA) is one of the most extensively studied plasma proteins due to its structural homology with human serum albumin (HSA), which plays an important role in the transport and deposition of endogenous and exogenous ligands in bovine blood, is a typical cofactor-free protein with multidomain structure [5]. As shown in Scheme 1, BSA consists of three homologous domains (I, II, and III) and each domain contains two subdomains (A and B) [6,7]. The domains were reported to have different lability to unfolding [8]. Therefore, the conformational changes of the domains in BSA are not synchronous, which makes the unfolding process of BSA more complex. A large variety of techniques have been developed to probe the folding/unfolding of BSA, such as fluorescence [9], circular dichroism (CD) [10], dynamic light scattering [11], UV–vis absorption [12], Fourier transform infrared [13], small-angle X-ray scattering [14], Raman [15], mass spectroscopy [16], nuclear magnetic resonance (NMR) [17], and electrochemistry [2]. Most of them only proposed a two-state transition [14–16]. The characterization of the intermediate state involved in the unfolding pathway of BSA is extremely difficult due to the lack of appropriate probes and methods [3]. Although three-state transition was revealed by CD and NMR, they are expensive and need extensive technical knowledge [17–19]. UV–vis spectroscopy is a very flexible technique that does not have special requirements. Electrochemical methods are also low cost, facile operation, rapidity with high sensitivity in probing the kinetic and thermodynamic information on protein unfolding [20,21]. However, because BSA has neither visible absorption nor redox-active cofactors, the elucidation of the folding/unfolding of BSA using UV–vis spectroscopy and electrochemistry is faint. Guo et al. [20] and Ahmad et al. [12] successively investigated the urea-induced unfolding of BSA by electrochemistry and UV difference spectroscopy respectively, but the intermediate state during the unfolding process is obscure.

Herein, the asynchronous structural transition of the domains in BSA during unfolding process was conveniently investigated by naked eyes, UV–vis spectroscopy and electrochemistry using a site-selective probe. Alizarin red S (ARS, Scheme 1) was selected as a site-selective probe to monitor the unfolding processes of BSA. The interaction parameters between ARS and BSA, including the

* Corresponding authors. Tel.: +86 020 84114919; fax: +86 020 84112901.
E-mail addresses: wuhai317@126.com (H. Wu), daizong@mail.sysu.edu.cn (Z. Dai), ceszxy@mail.sysu.edu.cn (X. Zou).

0039-9140/$ – see front matter.
doi:10.1016/j.talanta.2011.02.027

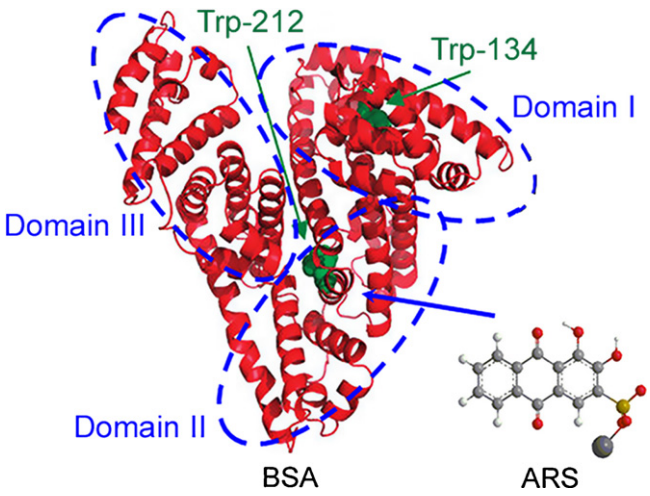

Scheme 1. Chemical structure and schematic domains of bovine serum albumin with tryptophan residues and the three-dimensional structure of alizarin red S.

binding constant, binding number, and binding mode, has been thoroughly explored by fluorescence, UV–vis spectroscopy and linear sweep voltammetry due to its possible cancer induction [22,23]. The exact binding site and binding process of ARS to BSA in view of the secondary structure of BSA has also been identified. According to fluorescence quenching techniques, ARS specifically binds to the subdomain IIA of BSA with the main acting forces of hydrogen bonds and van der Walls forces during the binding process (see details in SI, Figs. S1–S3). The formation of BSA–ARS complex caused the color change of solution from yellow to pinkish-red. As ARS located in domain II of BSA, the unfolding occurred in different domains caused different alterations of the microenvironment of ARS, resulting in distinguishable color changes. The conformational changes of domain III caused the rearrangement of domains I and II. The slight alteration of the microenvironment of ARS in domain II made the color of BSA–ARS become darker. In contrast, the unfolding taking place in domain II directly exposed the bound ARS to denaturing solution, causing the dissociation of ARS from BSA–ARS complex by the competition between denaturant and ARS. Thus, the original color of ARS was found in the bulk solution. Consequently, the dependent unfolding of the domains of BSA induced by denaturant was easily identified from the color change of bulk solution. Furthermore, because of the electroactivity of ARS, the changes in the microenvironment surrounding ARS caused different electrochemical responses, which allowed the investigation of the unfolding process of BSA through electrochemical technique. To our knowledge, it is the first report to realize the indicator of the intermediate state during the unfolding process of BSA through the convenient methods of naked eyes, UV–vis spectroscopy and electrochemical techniques, instead of expensive approaches. The work provides a facile method for the investigation of the unfolding process of multidomain proteins.

2. Materials and methods

2.1. Reagents and materials

BSA (MW 67000) and ARS were obtained from Sigma and used without further purification. All other chemicals were of analytical reagent grade and used as received. Acetate buffer solution (0.1 M) was prepared by mixing a stock solution of 0.2 M acetic acid, sodium acetate and sodium chloride, and the pH was adjusted to 5.05. Double-distilled water was used throughout. Aqueous solutions were prepared at ambient temperature.

2.2. Urea-induced unfolding of BSA–ARS

ARS was added dropwise into BSA solution in the molar ratio 1.5:1 to result in the formation of BSA–ARS complex. The solution of the complex was dialyzed to remove free ARS for 90 h in acetate buffer solution (0.1 M, pH 5.05) and the acetate buffer solution was refreshed once per 12 h. Then the same amount of BSA–ARS complex solution was added into the urea solutions with different concentrations for 12 h at 4 °C.

2.3. Apparatus and measurements

UV measurements were performed on a UV-3150 spectrophotometer (Shimadzu) using 1.0 cm quartz cells. Fluorescence spectra between 290 and 450 nm were recorded on a RF-5301PC spectrophotometer (Shimadzu) with a 1.0 cm quartz cuvette. The slit widths and the excitation wavelength were 5/5 nm and 280 nm, respectively.

Electrochemical experiments were performed with a CHI660C electrochemical workstation (Chenghua, Shanghai, China) equipped with a conventional three-electrode system. A glassy carbon electrode (GCE), 3 mm in diameter, was used as working electrode. A platinum wire and a Ag/AgCl electrode (3 M KCl) were used as counter and reference electrodes, respectively. Cyclic voltammetry was performed in the potential range from 0.8 to 0.3 V at a scan rate of 100 mV s^{-1}. All experiments were carried out at room temperature.

Circular dichroism (CD) measurements were carried out with a J-810 spectrometer in quartz cells (Tokyo, Japan). The CD spectra of ARS bound to BSA were recorded over a wavelength range of 200–250 nm with a scan speed of 50 nm min^{-1} and a band width of 1.0 nm. Each CD spectrum was the average of three scans. BSA was in pH 5.05 hydrochloric acid containing 0.1 M NaCl instead of acetate buffer solution in order to avoid the high absorbance of acetic acid in far ultraviolet.

3. Results and discussions

3.1. The specific interaction between ARS and BSA

ARS is an anthraquinone pigment with high affinity to BSA, which has both UV–vis adsorption and electroactivity and has the potential application as a visible and electrochemical probe for tracking the conformational transition of BSA.

As shown in Fig. 1Aa, 2.0 μM BSA in 0.1 M acetate buffer solution (pH 5.05) showed no UV–vis absorption from 300 to 700 nm, while ARS showed an obvious absorption peak at 422 nm (Fig. 1Ab), which was attributed to the absorption of anthraquinone chromophore. With the addition of BSA into ARS solution, a dramatic decrease of absorbance occurred with a red shift of absorption peak from 422 to 433 nm, and a new absorption peak at 535 nm appeared and increased gradually. A distinct isosbestic point was observed at 461 nm. The results indicate that a new complex forms in solution after the addition of BSA into ARS solution. The color of solution changed from yellow (ARS alone) to pinkish-red (BSA-ARS complex) (a and b in Fig. 1B).

Similar as UV–vis, the cyclic voltammograms (CVs) of ARS clearly showed the changes of its electroactivity during the formation of BSA–ARS complex with the addition of BSA. As shown in Fig. 1C, a pair of redox peaks were observed from 0.3 to 0.8 V when 0.2 mM ARS in 0.1 M acetate buffer solution (pH 5.05) was scanned electrochemically at GCE (Fig. 1C, curve a). According to the previous reports [24,25], the couple of redox peaks are assigned to the redox reaction of the side anthraquinone functionality of ARS. After additions of different concentrations of BSA into the ARS solution,

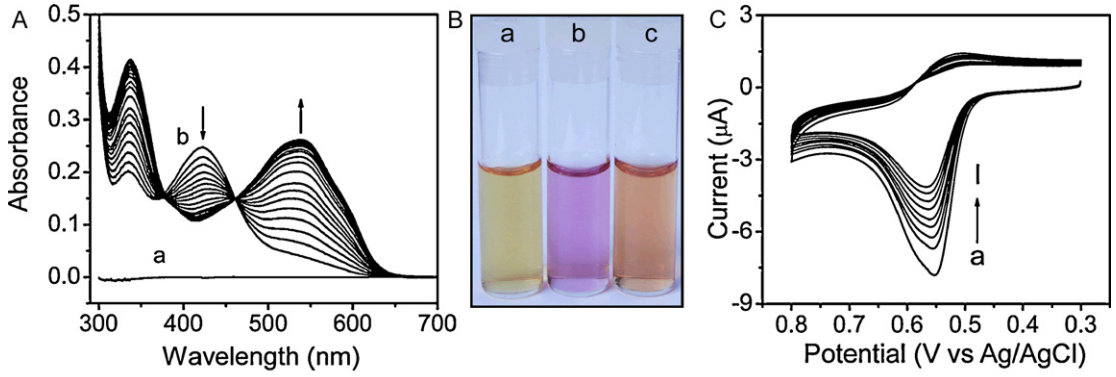

Fig. 1. (A) UV–vis spectra of 2.0 μM BSA (a) and 60.0 μM ARS (b) in 0.1 M acetate buffer solution (pH 5.05) upon the additions of BSA from 2.0 to 68.0 μM. (B) The corresponding colors of 60.0 μM ARS (a), 60.0 μM ARS in the presence of 68.0 μM BSA (b), and 60.0 μM ARS in acetate buffer solution containing 6.0 M urea (c). (C) CVs of ARS with different concentration of BSA in 0.1 M acetate buffer solution (pH 5.05) 0.2 mM ARS (a); 0.2 mM ARS in the presence of 0.02, 0.03, 0.04, 0.05, 0.06, 0.07, 0.08, 0.09 mM BSA (b → I).

the redox currents of ARS decreased significantly (Fig. 1C, curves b–e). According to Li et al. [26], the formation of a nonelectroactive complex between ARS and BSA resulted in the decrease of the peak currents of ARS.

As ARS specifically binds to BSA at subdomain IIA mainly through hydrogen bonds and van der Walls forces, the unfolding of BSA induced by denaturants, such as urea, acid and etc., changes the microenvironment surrounding the bound ARS and even dissociates ARS from BSA–ARS into bulk solution. Therefore, the change of spectral and electrochemical behaviors is in accordance with that of the color from the solution of BSA–ARS back to ARS. As shown in Fig. 1B, with the addition of urea to BSA–ARS complex solution, the pinkish-red color turned to orange gently (Fig. 1Bc, the color of ARS in urea is orange due to the increase of solution polarity). The results clearly indicate the possibility of investigation of BSA unfolding by visible, UV–vis spectral and electrochemical techniques.

It is known that the interaction between small molecules and proteins will cause the conformational changes of proteins [27]. Therefore, the secondary and tertiary structures of BSA after interacted with ARS were evaluated by far-UV CD and fluorescence spectra. Fig. 2A shows the CD spectra of BSA in the presence of ARS. Two negative peaks at 222 and 208 nm, which are assigned to the n–π^* transition of the carbonyl group and the parallel exactions of the π–π^* transition of peptide, respectively [28,29], were found to typically characterize the α-helices content of BSA. The negative peaks decreased slightly with the addition of ARS up to 2.0 μM (Fig. 2A), suggesting that the secondary structure was not greatly affected. Furthermore, the emission spectra of BSA decreased with no change in the maximum emission wavelength with the additions of ARS (Fig. 2B), indicating that the microenvironment of tryptophan (Trp) residues in BSA were not changed significantly. The tertiary structure of BSA remained unaltered after the binding of ARS [7,30]. Therefore, the three-dimensional structure of BSA–ARS complex was similar as that of BSA, and the unfolding process of BSA–ARS can be used to represent the unfolding of BSA.

3.2. Visible investigation of the urea-induced unfolding of BSA–ARS complex

Fig. 3 shows the changes of the UV–vis absorbance and the colors of BSA–ARS solution with the addition of urea from 0 to 8.0 M. When the concentration of urea increased from 0 to 4.0 M, the UV–vis absorbance at 530 nm increased, while the absorbance at 432 nm kept constant (a and b in Fig. 3A, and Fig. S5). Correspondingly, the pinkish-red color of BSA–ARS solution became darker gradually (from a to c in Fig. 3B). The results indicate that the domain III of BSA unfolds under these conditions. Because the stability of the domain III was lower than that of the domains I and II, the domain III was unfolded firstly under the inducement of urea, resulting in a partial loss of the native conformation of domain I, and a rearrangement of domains II and I [8]. The binding of ARS to the subdomain IIA of BSA was consequently improved, causing the increase of the absorbance of BSA–ARS complex. When the concentration of urea was in the range of 4.5–6.0 M, the UV–vis absorbance at 530 nm decreased, while the absorbance at 432 nm increased obviously (a and b in Fig. 3A). The color of BSA–ARS solution turned to orange (d and e in Fig. 3B), which was the color of ARS alone. The results suggested that the domain II of BSA started to unfold, causing the exposure of ARS to urea solution. The competitive hydrogen bond interactions between urea and ARS made ARS dissociate from BSA–ARS complex, leading to the loss of BSA–ARS complex and the increase of free-ARS in bulk solution. After the concentration of urea was higher than 6.0 M, no obvious absorbance change at 530 and 432 nm were observed (a and b in Fig. 3A, and Fig. S5), and the color of the solution fully changed into orange (f in Fig. 3B), which was exactly the same as that of ARS in 6.0 M urea (c in Fig. 1B). The results indicate that the total dissociation of ARS from BSA–ARS complex achieves and BSA is completely unfolded by urea. Therefore, the unfolding of BSA experienced an initial unfolding of domain III, followed with the rearrangement of domain I and II, and final unfolding of domain II. A two-step, three-state transition process was verified.

3.3. Electrochemical investigation of the urea-induced unfolding of BSA–ARS complex

BSA is a typical non-hemoprotein, which makes the electrochemical investigation of its unfolding extremely difficult. However, because of the electroactivity and site-selectivity of ARS, the unfolding of BSA can be easily monitored using ARS as an electrochemical probe. As shown in Fig. 4, the anodic peak current (I_{pa}) of BSA–ARS changed slightly with urea concentration up to 4.0 M (Fig. 4B). During this period, the pinkish-red color of solution became gradually darker (a in Fig. 4B), indicating the initial unfolding of domain III and a partial loss of the native conformation of domain I. The hydrophobic structure of domain II was inflected, which made the ARS buried in BSA easily be oxidized and therefore I_{pa} increased [21]. At the same time, the increase of the solution viscosity caused by urea decreased I_{pa}. As a result, I_{pa} almost kept constant. With increasing urea concentration from 4.0 to 6.0 M, an obvious increase of I_{pa} was obtained. The color of free-ARS in solution gradually appeared (b in Fig. 4B), indicating the dissociation of BSA–ARS occurred. Therefore, the increase of I_{pa} was the result of the increased amount of free ARS in solution. When the concentra-

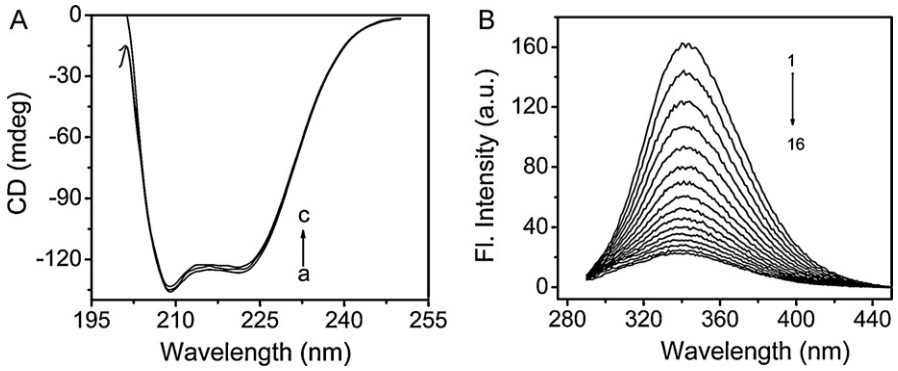

Fig. 2. (A) The CD spectra of 1.0 μM BSA in 0.1 M NaCl solution with 0 (a), 1.0 (b) and 2.0 μM (c) ARS; (B) fluorescence spectra of 2.0 μM BSA in 0.1 M pH 5.05 acetate buffer solution with the addition of 0.0, 0.4, 0.8, 1.2, 1.6, 2.0, 2.4, 2.8, 3.2, 3.6, 4.0, 4.4, 4.8, 5.2, 5.6, 6.0 μmol L^{-1} ARS (curves 1–16). (T = 293 K, and λ_{ex} = 280 nm).

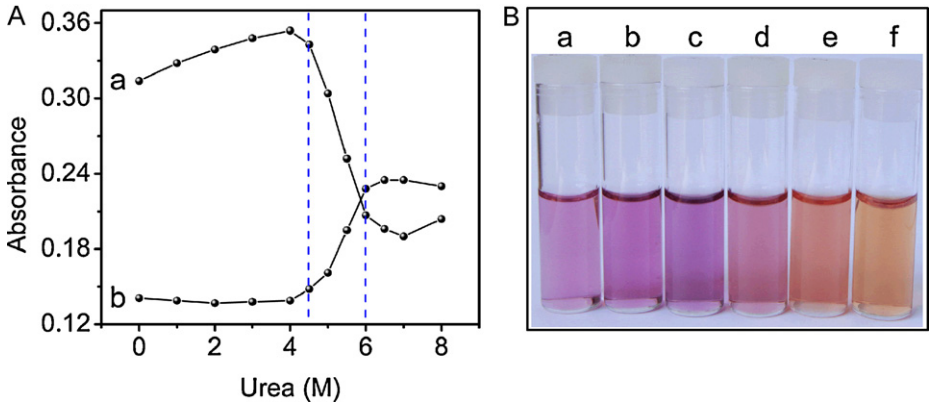

Fig. 3. (A) UV–vis absorbance intensity of 61.0 μM BSA–ARS in 0.1 M acetate buffer solution with various urea concentrations. UV–vis absorbance at 530 nm (a) and 432 nm (b); (B) the corresponding colors of BSA–ARS complex solutions with urea concentrations of 0 (a), 2.0 (b), 4.0 (c), 5.0 (d), 6.0 (e), and 8.0 M (f).

tion of urea was higher than 6.0 M, I_{pa} kept constant and the color of solution fully turned to be orange (c in Fig. 4B). The complete unfolding was achieved and the amount of free-ARS in bulk solution did not change significantly. In comparison with the method by the catalytic oxidation of the tyrosine (Tyr) and Trp residues in BSA [20], the catalytic voltammetry depended on the permeability of the electron mediator inside the BSA and mainly reflected the conformational changes around Tyr and Trp. The proposed method was based on the site-selective binding of ARS to domain II of BSA. Therefore, the unfolding of domain III in BSA only caused a slight change of the voltammetric response of BSA–ARS, while the unfolding of domain II led to an extreme increase of current response due to the dissociation of ARS from BSA–ARS complex. Consequently, the asynchronous structural transition of the domains in BSA could be clearly and sensitively identified by the current alteration.

3.4. Verification of the unfolding process of BSA by fluorescence spectroscopy

BSA has two Trp residues. Trp-134 is in the subdomain IB and Trp-212 is in the subdomain IIA [31,32]. The change of the intrinsic fluorescence from Trp residues in BSA can be used to reflect the conformational transition of BSA. As shown in Fig. 5A and Fig. S6, the fluorescence of BSA–ARS decreased gradually with blue shift at 342 nm as increasing the concentrations of urea from 0 to 4.5 M. According to the results from visible method mentioned above, the

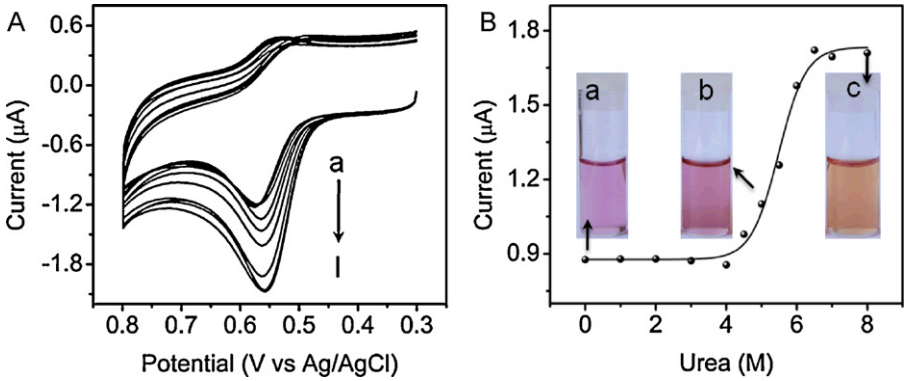

Fig. 4. (A) Cyclic voltammograms of 61.0 μM BSA–ARS in 0.1 M acetate buffer solution (pH 5.05) with the addition of urea concentrations of 0 (a), 1.0 (b), 2.0 (c), 3.0 (d), 4.0 (e), 4.5 (f), 5.0 (g), 5.5 (h), 6.0 (i), 6.5 (j), 7.0 (k), and 8.0 M (l) at the scan rate of 100 mV s^{-1}. (B) The plots of the I_{pa} *vs.* urea concentrations and the corresponding colors of BSA–ARS complex solutions with urea concentrations of 0 (a), 5.0 (b), and 8.0 M (c).

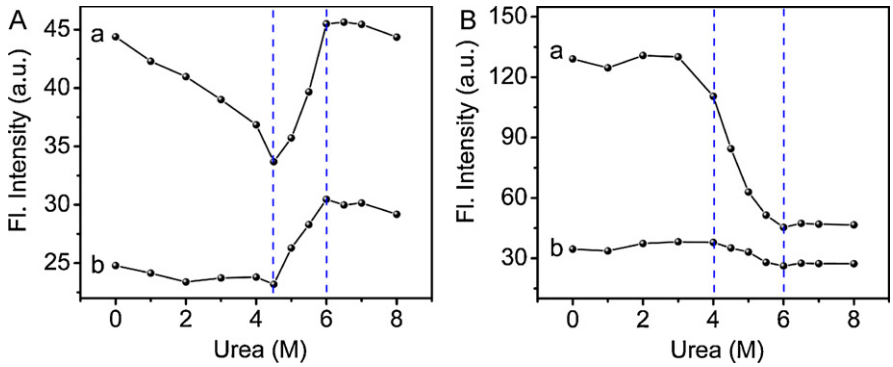

Fig. 5. Intrinsic fluorescence intensity of 61.0 μM BSA–ARS (A) and BSA (B) in 0.1 M acetate buffer solution with various urea concentrations. Fluorescence intensity at 342 nm (a) and 310 nm (b) with excitation wavelength of 280 nm.

domain III of BSA started to unfold under these conditions, leading to the rearrangement of domain II and partial domain I. Therefore, the decrease in fluorescence intensity at 342 nm (a in Fig. 5A) was caused by the improvement of the fluorescence quenching between ARS and Trp-212, and the blue shift of Trp fluorescence was the results from the interaction between the backbone of BSA and urea through hydrogen bond, electrostatic interactions and van der Waals attractions [33,34]. After further increasing the urea concentration from 4.5 to 6.0 M, the fluorescence at 342 nm increased noticeably with red shift. At the same time, a shoulder peak at 310 nm, which was attributed to the fluorescence of Tyr residues, appeared and got stronger (b in Fig. 5A, and Fig. S6). At these conditions, the domain II started to unfold, causing the dissociation of ARS from BSA–ARS. Therefore, the distance between Tyr and Trp residues increased, leading to the decrease of the energy transfer among ARS, Tyr and Trp. Thus, the fluorescence intensities of Trp and Tyr were both enhanced (a and b in Fig. 5A) [30,35]. The exposure of Trp to polar environment also caused the red shift of Trp fluorescence due to the loss of the compact structure of the hydrophobic domain II. When the concentration of urea was higher than 6.0 M, the fluorescence intensities at 342 and 310 nm kept no obvious change (a and b in Fig. 5A). The results were well in agreement with the observations from the visible method.

Similar as BSA–ARS complex, the unfolding of BSA induced by urea was also tested directly by fluorescence spectroscopy. As shown in Fig. 5B and Fig. S7, the changes of fluorescence intensity appeared obviously different from those of BSA–ARS complex. The fluorescence intensity of BSA showed no significant change at urea concentrations between 0 and 4.0 M, and decreased from 4.0 to 6.0 M (a and b in Fig. 5B). The reasons were that the initial unfolding of the domain III in BSA did not cause significant changes of the hydrophobic environment around Trp and Tyr before 4.0 M urea, while the unfolding of domain II beyond 4.5 M urea brought Trp-212 to be more exposed to a more polar environment, allowing water molecules or other amino acid residues to quench the fluorescence [36,37]. The results indicate that BSA–ARS complex has the same unfolding process as BSA, but the sensitivity of probing the unfolding process is extremely enhanced by using the site-selective probe of ARS.

4. Conclusions

ARS was used as a site-selective probe to monitor the asynchronous unfolding processes of BSA in aqueous solution. Based on the visualization of color changes, spectral and electrochemical responses, the unfolding process of BSA was verified to undergo from the initial unfolding of domain III, followed with the rearrangement of domain I and II, and final unfolding of domain II. Through the use of the dual properties site-selective probe, the proposed method can be conveniently used to estimate the unfolding procedures of other colorless or cofactor-free multidomain proteins.

Acknowledgments

We gratefully acknowledge financial support from the National Natural Science Foundation of China (Nos. 20805059, 20975117), the Natural Science Foundation of Guangdong Province (10151027501000070), the Scientific Technology Project of Guangdong Province (No. 2010A040302001), the Scientific Research Foundation for the Returned Overseas Chinese Scholars of State Education Ministry, the Ph.D. Programs Foundation of Ministry of Education of China (No.20070558010), and the Fundamental Research Funds for the Central Universities (10lgzd13).

Appendix A. Supplementary data

Supplementary data associated with this article can be found, in the online version, at doi:10.1016/j.talanta.2011.02.027.

References

[1] E. Pinho Melo, M.R. Aires-Barros, S.M.B. Costa, J.M.S. Cabral, J. Biochem. Biophys. Methods 34 (1997) 45–59.
[2] M. Chiku, J. Nakamura, A. Fujishima, Y. Einaga, Anal. Chem. 80 (2008) 5783–5787.
[3] K.E. Amunson, L. Ackels, J. Kubelka, J. Am. Chem. Soc. 130 (2008) 8146–8147.
[4] Y.N. Hong, C. Feng, Y. Yu, J.Z. Liu, J.W.Y. Lam, K.Q. Luo, B.Z. Tang, Anal. Chem. 82 (2010) 7035–7043.
[5] Z.M. Wang, Z.H. Song, D.H. Chen, Talanta 83 (2010) 312–319.
[6] V.S. Jisha, K.T. Arun, M. Hariharan, D. Ramaiah, J. Am. Chem. Soc. 128 (2006) 6024–6025.
[7] D.M. Charbonneau, H.-A. Tajmir-Riahi, J. Phys. Chem. B 114 (2010) 1148–1155.
[8] S. Tayyab, N. Sharma, M.M. Khan, Biochem. Biophys. Res. Commun. 277 (2000) 83–88.
[9] S. Ghosh, N. Guchhait, ChemPhysChem. 10 (2009) 1664–1671.
[10] R. Ghosh, S. Sharma, K. Chattopadhyay, Biochemistry 48 (2009) 1135–1143.
[11] S. Chodankar, V.K. Aswal, J. Kohlbrecher, R. Vavrin, A.G. Wagh, Phys. Rev. E 77 (2008) 031901–31911.
[12] N. Ahmad, M.A. Qasim, Eur. J. Biochem. 227 (1995) 563–565.
[13] V. Militello, C. Casarino, A. Emanuele, A. Giostra, F. Pullara, M. Leone, Biophys. Chem. 107 (2004) 175–187.
[14] C. Leggio, L. Galantini, P.V. Konarev, N.V. Pavel, J. Phys. Chem. B 113 (2009) 12590–12602.
[15] C. David, S. Foley, C. Mavon, M. Enescu, Biopolymers 89 (2008) 623–634.
[16] O. Azim-Zadeh, A. Hillebrecht, U. Linne, M.A. Marahiel, G. Klebe, K. Lingelbach, J. Nyalwidhe, J. Biol. Chem. 282 (2007) 21609–21617.
[17] C.X. Sun, J.H. Yang, X. Wu, X.R. Huang, F. Wang, S.F. Liu, Biophys. J. 88 (2005) 3518–3524.
[18] C.T. Lee, K.A. Smith, T.A. Hatton, Biochemistry 44 (2005) 524–536.
[19] A. Domínguez-Vidal, M.P. Saenz-Navajas, M.J. Ayora-Cañada, B. Lendl, Anal. Chem. 78 (2006) 3257–3264.
[20] L.H. Guo, N. Qu, Anal. Chem. 78 (2006) 6275–6278.
[21] X.C. Li, W. Zheng, L.M. Zhang, P. Yu, Y.Q. Lin, L. Su, L.Q. Mao, Anal. Chem. 81 (2009) 8557–8563.

[22] F. Ding, J.L. Huang, J. Lin, Z.Y. Li, F. Liu, Z.Q. Jiang, Y. Sun, Dyes Pigments 82 (2009) 65–70.
[23] W. Sun, K. Jiao, Talanta 56 (2002) 1073–1080.
[24] V.E. Mouchrek Filho, A.L.B. Marques, J.J. Zhang, G.O. Chierice, Electroanalysis 11 (1999) 1130–1136.
[25] H.P. Dai, K.K. Shiu, Electrochim. Acta 43 (1998) 2709–2715.
[26] Z.W. Zhu, N.Q. Li, Microchim. Acta 130 (1999) 301–308.
[27] T.Q. Wu, Q. Wu, S.Y. Guan, H.X. Su, Z.J. Cai, Biomacromolecules 8 (2007) 1899–1906.
[28] A. Divsalar, M.J. Bagheri, A.A. Saboury, H. Mansoori-Torshizi, M. Amani, J. Phys. Chem. B 113 (2009) 14035–14042.
[29] K. Matsuura, T. Saito, T. Okazaki, S. Ohshima, M. Yumura, S. Iijima, Chem. Phys. Lett. 429 (2006) 497–502.
[30] P. Qu, H. Lu, X.Y. Ding, Y. Tao, Z.H. Lu, Spectrochim. Acta Part A 74 (2009) 1224–1228.
[31] B. Ojha, G. Das, J. Phys. Chem. B 114 (2010) 3979–3986.
[32] Y.N. Li, G.L. Liu, S. Kokot, Talanta 76 (2008) 513–521.
[33] L. Galantini, C. Leggio, P.V. Konarev, N.V. Pavel, Biophys. Chem. 147 (2010) 111–122.
[34] A. Caballero-Herrera, K. Nordstrand, K.D. Bernt, L. Nilsson, Biophys. J. 89 (2005) 842–857.
[35] A. Sułkowska, J. Równicka, B. Bojko, J. Pożycka, I. Zubik-Skupień, W. Sułkowski, J. Mol. Struct. 704 (2004) 291–295.
[36] D.M. Togashi, A.G. Ryder, D. O' shaughnessy, J. Fluoresc. 20 (2010) 441–452.
[37] W. Qiu, T. Li, L. Zhang, Y. Yang, Y.T. Kao, L. Wang, D. Zhong, Chem. Phys. 350 (2008) 154–164.